

UDC 543.544.25+519.242.5

Intermetallic Compounds as Highly Active Catalysts for Natural Gas Conversion

L. A. ARKATOVA

Tomsk State University,
Pr. Lenina 36, Tomsk 634050 (Russia)

E-mail: larisa-arkatova@yandex.ru

Abstract

The method of self-propagating high temperature synthesis was used for preparing highly efficient catalysts from Ni–Al alloys corresponding to the basic composition of Ni₃Al intended for the process of carbon dioxide methane conversion. A low-dose modifying of platinum was carried out using ion implantation. Catalysts were tested in the course of carbon dioxide methane conversion at an atmospheric pressure and within the temperature range of 600–900 °C. It is demonstrated that the microstructure of the samples exerts a significant effect on the catalytic activity and stability of their functioning. A maximum activity is inherent in nanostructured catalysts those represent Pt clusters with size ranging from 0.3–0.5 to 3–5 nm, stabilized within the structure of intermetallic compound Ni₃Al and Al₂O₃. Using the methods of XRD, SEM, EDS, HRTEM, XPS, DSC-TG it was demonstrated that unmodified catalysts undergo a partial coking in the course of methane conversion into synthesis gas, whereas samples modified with platinum are stable and almost non-affected by deactivation due to carbonization.

Key words: methane conversion into synthesis gas, intermetallic compounds, self-propagating high temperature synthesis, ion implantation

INTRODUCTION

The rapid development of science and technology puts to the forefront a problem of developing the materials with specific, often unique properties. A great potentiality in this area is exhibited by intermetallic compounds [1]. Among them, there are compounds with a low temperature of formation and melting, semiconductors and superconductors, compounds with high strength and oxidation resistance at elevated temperature values as well as with a unique property of «memory effect». Currently, these materials are increasingly being used for practical purposes (in electrical engineering, electronics, semiconductor industry, nuclear energy as well as for creating the products of new technologies and protective coatings for novel equipment). The feature of intermetallic compounds consists in the fact that they can exist in crystalline form only, that one cannot distinguish individual molecules therein, that they could not be melted or dis-

solved without loss of individuality and that they do not exist in the gas phase.

These compounds exhibit specific metallic properties, whereas their physicochemical properties differ to a considerable extent from the properties of the components and the properties of intermetallic compounds with the same elemental composition, but with a different componential ratio. Owing to the peculiarities of the crystal and electronic structure of intermetallic compounds, they demonstrate an optimization of properties important for practical application. Thermal stability, mechanical strength and high thermal conductivity inherent in nickel aluminides results in growing interest in the potentialities of their use as catalysts or carriers for an active component in the reactions with significant thermal effects, for example in the processes of natural gas (methane) conversion, which is especially important for Russia and Russian regions with a considerable reserves of this raw material [2, 3].

The extent of natural gas chemical processing is constrained primarily by the fact that almost all the pathways of its transformation into valuable chemical products implemented on an industrial scale are based on a complex energy- and capital-intensive process of natural gas pre-conversion into the synthesis gas [4]. In this connection, it is necessary to conduct research work aimed at developing high-efficiency catalysts for catalytic oxidation of methane into synthesis gas; those promote decreasing energy consumption value in large-tonnage processing of natural gas.

Among different methods of obtaining the synthesis gas there is methane steam conversion (MSC) only that is widely used in industrial scale [4]:



However, taking into account the disadvantages of this method (a high cost of superheated steam, the evolution of excess CO_2 in significant amounts, a componential ratio $\text{H}_2/\text{CO} = 3 : 1$ inconvenient for obtaining liquid hydrocarbons *via* the Fischer-Tropsch process as well as other valuable products of chemical and petrochemical industry) the development of alternative methods for obtaining the synthesis gas is currently important.

Carbon dioxide methane conversion (CDMC):



is not implemented on an industrial scale. Just as the steam reforming, it represents an endothermic process, whereas the cost of industrial realizing the two processes is incommensurable [4]. At the same time, the carbon dioxide methane conversion results in the formation of synthesis gas with low $n(\text{H}_2)/n(\text{CO})$ ratio in the products, which is optimal for obtaining dimethyl ether (as a promising environmentally safe fuel), as well as for realizing the oxosynthesis [4, 5]. The advantages of CDMC consist also in the fact that the process utilizes two gases (CO_2 and CH_4) causing the greenhouse effect.

According to the forecasts of the International Energy Agency, the predominant source of energy in the 21st century should be presented by fossil fuel species, so that the CO_2 emissions into the atmosphere in 2020 would exhibit a 50 % increase compared to the level observed in 1990 [6]. Limiting carbon dioxide emissions is currently one of the most ambi-

tious tasks of the catalysis. A high value of the enthalpy of endothermic methane reforming reaction under the influence of CO_2 and the ability of the reverse conversion cause the process to be one of the most suitable for the storage of renewable energy sources.

In the catalytic studies aimed at studying the mentioned reaction, the main attention is paid to the following specific aspects: the activity of proper the metallic phase and its resistance with respect to the carbon deposits as well as to the choice of media which promotes to improve the efficiency of the catalyst [6–8].

Nickel catalysts have proven to be promising in this reaction, and their activity is comparable to the activity of noble metals [7–10]. As a rule, nickel is applied onto a variety of materials such as Al_2O_3 [7], MgO and TiO_2 [4, 8], *etc.* However, the most of catalysts are subjected to relatively rapid deactivation caused by coke formation [3–5]. Modifying the catalysts enhances the activity and reduces the amount of carbon on their surface [11, 12].

The aim of this work consisted in developing novel materials implanted with platinum as the active and stable catalysts for carbon dioxide methane reforming basing on intermetallic compound Ni_3Al .

EXPERIMENTAL

Ni-containing catalysts based on Ni–Al alloys were prepared from commercial samples of nickel (PNE-1) and aluminium (ASD-4) metals; those were previously exposed to drying in vacuum at 100 °C for 4 h. The samples were then thoroughly mixed and pressed to form cylindrical workpieces for obtaining the optimum density affecting the course of the synthesis process [1]. The method of preparation consisted in self-propagating high temperature synthesis (SPHTS) with using a layer-by-layer combustion mode, taking into account Ni–Al phase diagram [13]. The porosity of the samples, which characterizes the density of the mixture, was calculated using the formula

$$\eta = (d_c - d_p)/d_c \cdot 100 \%$$

Here η is the initial porosity of the sample, %; d_c is the density of the compacted material, g/cm^3 ; d_p is the density of the pressed sample, g/cm^3 .

The synthesis was carried out in a constant pressure bomb within the environment of an inert gas (argon), where at first we performed an initiation of the combustion of pressed workpieces by means of a thermal pulse from a tungsten spiral, and further the wave front spontaneously propagated along the axis of a workpiece. After cooling in an inert environment, the rod obtained was grinded; for catalytic studies we selected the fraction with the particle sizes within the range of 1000–600 μm , for each of the systems obtained.

Platinum modification was carried out *via* ion implantation performed using a vacuum-arc ion source in an improved apparatus developed at the Lawrence National Laboratory (Berkeley, USA, Mevva sources) [14]. The implantation conditions were as it follows: ion current density 2.3 mA/cm², average ion energy 60 keV, dose $1 \cdot 10^{17}$ ions/cm², frequency 2 Hz, vacuum $3 \cdot 10^{-6}$ Torr.

The phase composition of the samples before and after catalytic testing was determined by means of X-ray diffraction analysis on a Shimadzu XRD-6000 diffractometer with $\text{CuK}\alpha$ radiation, $\lambda = 0.154187$ nm (database: PCPDF-WIN and POWDER CELL 2.4.). Also, powder diffraction patterns of catalysts were recorded using a Siemens D-501 goniometer equipped with a Johansson monochromator focusing $\text{K}\alpha$ radiation with a low background and high resolution.

Catalytic testing was carried out with the use of a flow-through apparatus with a quartz tube reactor 5 mm in diameter with a fixed catalyst bed. The analysis of initial reactants and reaction products was carried out using a Chromos GC 1000.1 chromatograph. As a sorbent, we used Carbosieve S II for the determination of CH_4 , C_2H_6 , CO_2 , C_2H_4 , C_3H_8 , C_3H_6 , H_2O , N_2 , H_2 , CO . The conditions of chromatographing were as it follows: the rate of carrier gas (helium) 30 mL/min, steel column 3 m long and with an inner diameter of 3 mm, the analysis time was equal to 20 min with a programmed heating from 40 to 225 °C. In order to calculate the concentration of gaseous reaction products we used the method of absolute calibration. The morphology of catalysts was studied using scanning electron microscopy (SEM) on a VegaII LMU electron microscope (Czech Republic) with

an X-ray energy dispersion microprobe system Oxford INCA Energy 350 integrated with VegaII LMU. All the micrographs were made under high vacuum conditions, with the primary electron beam energy of 20 kV and with the use of a secondary electron detector in a “permission” mode.

The investigation of the carbonization level of the catalysts were performed using a Netzsch STA 409 synchronous thermal analysis instrument (Germany) which combines simultaneous thermogravimetry and differential scanning calorimetry (DTA/DSC integrated with a QMS 403 mass spectrometer (Germany). The temperature range of the oxidative treatment of catalysts amounted to 25–1100 °C; the heating rate was equal to 10 °C/min in air flow.

The microstructure of the catalysts was studied using the method of high resolution transmission electron microscopy (HRTEM) on a JEM-2010 transmission electron microscope at the accelerating voltage of 200 kV and the resolution equal to 1.4 Å. The catalyst particles were deposited dispersing an ethyl alcohol sample suspension onto a copper substrate using an ultrasonic disperser. Local analysis of the elemental composition of the samples was performed using an EDAX-Phoenix energy dispersion spectrometer with Si(Li) detector, with the energy resolution better than 130 eV. The lattice parameters and interplanar distances were determined *via* fast Fourier transform using Gatan Digital Micrograph 3.3.1 software.

XPS spectra were obtained by means of a Physical Electronic 5700 spectrometer equipped with a hemispherical electron analyzer and an X-ray excitation source $\text{MgK}\alpha$ (1253.6 eV, 15 kV, 300 W). Calibration was carried out according to C1s line (284.4 eV) with a deviation of ± 0.2 eV. The samples were placed into vacuum (10^{-9} Torr); in order to avoid the reduction of metals the time of sample irradiation was minimized. Because of signal asymmetry we performed spectral band deconvolution, and in all the cases appropriate Lorentz–Gaussian mathematical functions (80–20 %, respectively) were fitted for corresponding signals, with a maximum deviation value χ^2 .

RESULTS AND DISCUSSION

Catalytic activity

Preliminary tests of a series of catalysts based on Ni–Al alloys with varying nickel content (92.5–86.6 %) and aluminium content (7.5–13.4 %) demonstrated that among the intermetallic compounds under investigation, the system with superstoichiometric nickel content (92.5 mass % Ni and 7.5 mass % Al) regarding to the phase Ni₃Al, where a different Ni/Al mass ratio value takes place (86.6 : 13.4 mass %), is most active in the reaction of CDMC [3]. However, despite the good catalytic properties, the system was subjected to a partial deactivation due to carbonization. In this regard, taking into account a high activity in CDMC and coke resistance of precious metals, we used platinum in order to modify the intermetallic compounds based on Ni₃Al. Because of a relatively high cost of the metal, we used ion implantation technique that allowed us to modify the intermetallide with platinum, with platinum mass fraction less than 0.1 %. Moreover, in order to increase contact resistance with respect to carbon deposition, the modification of intermetallic Ni–Al matrix was performed using a composition with the ratio Ni/Al = 86.6 : 13.4 mass %. In other words, in order to avoid synthesizing a sample with an excess nickel phase content provoking coal formation, we choose a stoichiometric composition.

Effect of temperature. The reaction of dry methane reforming was studied in the presence of the two catalysts: Ni₃Al (taking into account the maximum activity of the chosen sample with the ratio Ni : Al = 92.5 : 7.5 mass % and Ni₃Al intermetallide implanted with Pt at a dose of 1017 ions/cm². The total flow rate of reagent mixture (CH₄/CO₂/He = 20 : 20 : 60 vol. %) was equal to 100 mL/min, the volume of catalyst amounted to 1 cm³. Figure 1 demonstrates the temperature dependence of methane and carbon dioxide conversion level values at both contacts.

At moderate temperature (500–550 °C), moderate values of the conversion level (ca. 25–32 %) are reached only for the implanted catalyst. In this case, as demonstrated in additional experiments, the conversion level is proportional

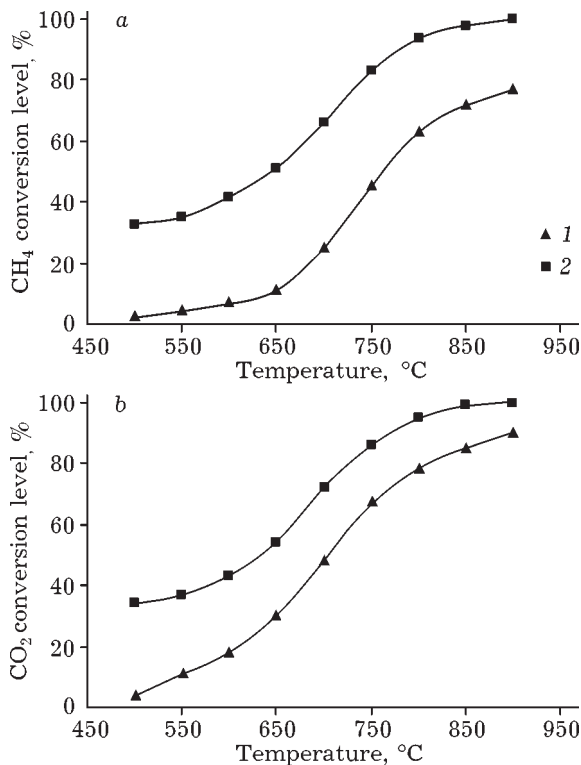
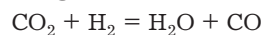


Fig. 1. Methane (a) and carbon dioxide (b) conversion level depending on temperature for the catalysts Ni₃Al (1) and Ni₃Al + Pt (2). Here and in Figs. 2, 3, and 7: pre-treatment – heating in the flow of helium up to 600 °C; temperature range equal to 600–900 °C; CO₂/CH₄/He = 20 : 20 : 60 vol. %; volumetric raw supply flow rate amounting to 100 cm³/min; the catalyst volume equal to 1 cm³.

to the dose of implanted platinum. As the temperature increased the methane and carbon dioxide conversion level exhibit an increase, which confirms the endothermic nature of the reaction (2). These two reagents, to all appearance, promote the mutual dissociation of each other [6].

As demonstrated by the results obtained at 850–900 °C, intermetallides based on Ni₃Al matrices are efficient catalysts for methane reforming with carbon dioxide. So, the conversion level $x(\text{CH}_4)$ and $x(\text{CO}_2)$ for the unmodified catalyst are equal to 76 and 82 %, respectively. After modifying by platinum, even at extremely low content of it (less than 0.1 mass %), these values already reached 97 and 99 %, respectively. When reforming an equimolar mixture of CO₂ and CH₄, the conversion level of both reactants must be the same [4–6]. However, for the catalysts investigated in this work the conversion level $x(\text{CO}_2)$ exceeded the con-

version level $x(\text{CH}_4)$. So, at 800 °C for Ni_3Al , these values were equal to 73 and 64 %, respectively, whereas for the $\text{Ni}_3\text{Al} + \text{Pt}$ the conversion level was 95 and 92 %, respectively. This could be explained by the fact that the main reaction (2) under the experimental conditions is accompanied by several secondary reactions [5, 6]. For example, by the reaction of reverse water gas shift (RWGS):



Some authors attribute this discrepancy to a complete dissociation of carbon dioxide according to the reactions [6]



Effect of CH_4/CO_2 molar ratio. It was demonstrated that the composition of the reaction mixture to a considerable extent affects the conversion level of CO_2 and CH_4 . For example, increasing the ratio of CO_2 and CH_4 from 1 to 3 the methane conversion level increases from 64 to 78 %, respectively, at the temperature of 800 °C. In contrast, the conversion level of carbon dioxide is reduced from 73 to 36 %. At the same time the carbon balance is improved in proportion as the reaction mixture is enriched with carbon dioxide. At $\text{CO}_2/\text{CH}_4 = 1 : 1$ the conversion level for CO_2 is equal to 78 %, whereas at $\text{CO}_2/\text{CH}_4 = 3 : 1$ this value amounts to 87 %. A favourable effect of CO_2 on the process

of CDMC is caused by its ability to regenerate coked catalysts with the formation of CO and CH_4 according to the mechanism of hydrogen disproportionation [16].

Basing on the catalytic data one could conclude that modifying the intermetallic compound Ni_3Al with extremely small platinum doses promotes a significant increase in the activity of the samples in the course of carbon dioxide methane conversion.

Phase composition

Sample Ni_3Al (92.5 mass % Ni and 7.5 mass % Al). Figure 2 demonstrates XRD patterns of catalysts both freshly prepared and developed under CDMC (900 °C, 24 h). For the reliable identification of the data obtained we demonstrate diffraction patterns of phases proposed: Ni_3Al , Ni, $\text{Ni}_{1.04}\text{Al}_{0.96}$, $\text{Ni}_{0.9}\text{Al}_{1.1}$, Ni_2Al_3 (according to the Crystallographica Search-Match Database, CSM DB).

It is seen that the main phase, both before and after testing in the course of CDMC, is presented by Ni_3Al . Distinctly pronounced superstructure reflections from crystallographic planes (100) and (110) in the angular range $23^\circ < 2\theta < 37^\circ$ indicate the formation of a long-range order in the crystal lattice of the inter-

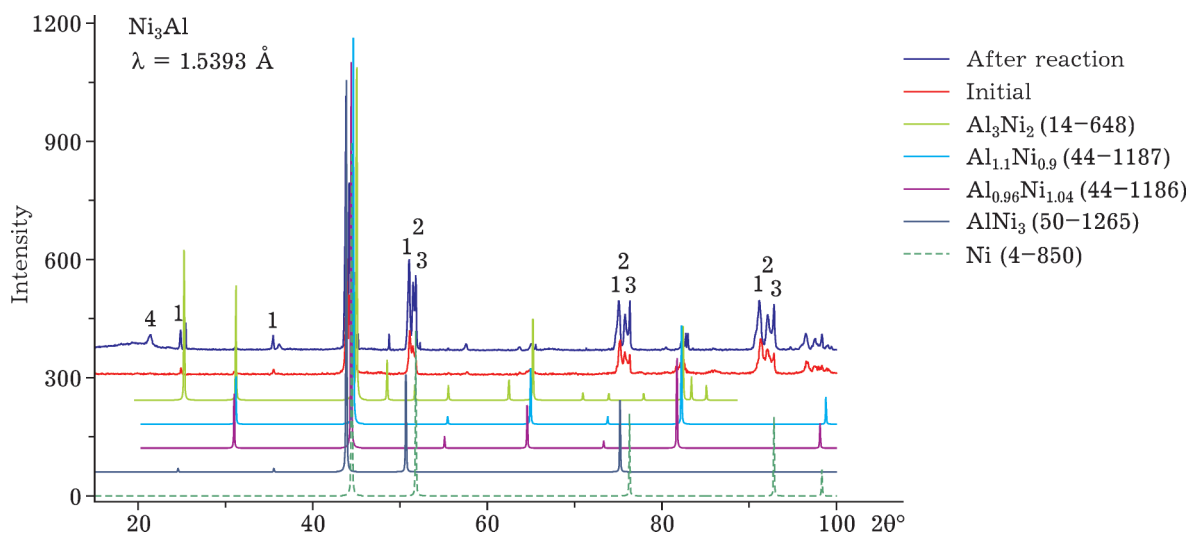


Fig. 2. Diffraction patterns for the samples of Ni_3Al based catalysts – initial and developed in the course of CDMC (for the process conditions see Fig. 1) in comparison with the diffraction patterns according to Crystallographica Search-Match DB. Phases: 1 – Ni_3Al , 2 – an ordered solid solution of Al in Ni, 3 – Ni, 4 – C (graphite).

metallide, although in the course of the SPHTS the process of Ni dissolution in Al is interfered by a chemical reaction between the compounds. Thus, the two processes occur simultaneously: such as the growth of an intermetallic compound layer due to the processes of diffusion, and the reaction of its dissolution. Even for the already existing phase Ni_3Al at high temperature values, an ordering determined by the first order phase transition is realized with the alloy segregation and the region of two-phase equilibrium [17]. Self-ordering does not occur uniformly, but in a fluctuation-like manner, and first locally ordered regions, antiphase domains are formed, whereas the further ordering is realized as the result of the growth of these domains. For this reason, the formation of the solid solution of Al in Ni under natural conditions of CDMC is in accordance with the laws of nature, and the further segregation of nickel occurs just from this solution.

Thus, comparing the theoretical and experimental diffraction patterns for the different compounds in the Ni–Al system (see Fig. 2) one could conclude that, in addition to intermetallic Ni_3Al , the phase of metallic Ni, as well as that of the ordered solid Al solution in Ni are detected. In addition, within the range of small diffraction angles a diffuse peak ($17\text{--}25^\circ$) is observed, suggesting the presence of amorphous carbon, and a quite distinct reflex of the phase of graphite ($\sim 23^\circ$).

Analyzing the diffraction patterns of the CDMC developed sample we revealed that the Ni_3Al phase still dominates, but its relative intensity decreases, whereas for the Ni phase we observed an increase in the intensity. It could be assumed that a part of the intermetallic compound decomposed with the formation of metallic nickel phase in the course high temperature treatment in an aggressive environment of the CDMC process, which nickel is represents an active centre for methane and carbon dioxide activation [4, 5]. Thus, the role of Ni_3Al intermetallic compound consists in stabilizing the structure of the catalytic system, since this intermetallide belongs to the category of superalloys with self-ordering structure and exhibits an abnormally high mechanical strength, thermal conductivity and heat resistance, and

therefore it represents a worthy competitor of the oxide ceramics.

Sample of $\text{Ni}_3\text{Al} + \text{Pt}$. Figure 3 demonstrates the XRD patterns of freshly prepared and CDMC developed (900°C , 24 h) catalysts. For comparison, data for “native” matrix are presented, where to the implantation was performed, *i. e.*, Ni_3Al (86.6 mass % Ni and 13.4 mass % Al).

According to Fig. 3, *a, b*, the initial sample is almost single-phase and represents Ni_3Al intermetallic compound. At the same time reflexes are rather broad, so there could be a very small amount of nickel phase, taking into account very close Ni_3Al and Ni lattice parameters, as well as a slight asymmetry of weak reflexes, for example, those from crystallographic planes (111) within the range of $2\theta = 44.2^\circ$. After the catalytic experiments, the dynamics of phase formation is similar to the unmodified sample, *i. e.*, there was a partial destruction of the intermetallic compound Ni_3Al phase with the release of free Ni phase and of an ordered solid solution of Al in Ni observed. No phases of graphite and amorphous carbon

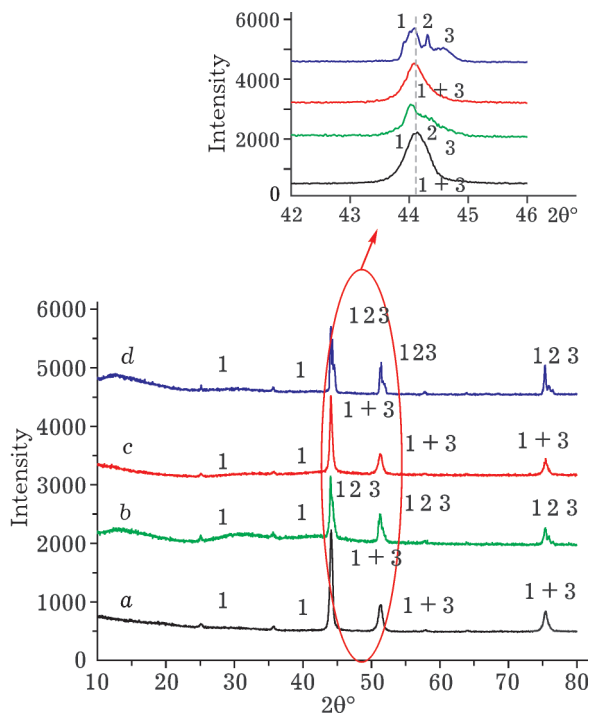


Fig. 3. Diffraction patterns for the samples of catalysts: *a, b* – matrix Ni_3Al (*a* – initial, *b* – after catalytic test in the course of CDMC); *c, d* – $\text{Ni}_3\text{Al} + \text{Pt}$ (*c* – initial, *d* – after catalysis; for the process conditions see Fig. 1); phases: 1 – Ni_3Al , 2 – solid solution of Al in Ni, 3 – Ni.

were found, which is confirmed by the results of DTA–TG. No platinum reflexes were registered, too, which can be explained by a highly dispersed state of platinum resulted from the ion-plasma impact on the surface of the sample.

It should be noted that the lattice parameter of Ni_3Al increases smoothly (from 0.3574 to 0.3580 nm) compared to the ideal value (0.3572 nm, according to CSM DB) with an increase in the working time of the catalyst. This could be caused by the bulk diffusion of carbon atoms formed, for example, as the result of the dissociative adsorption of methane.

Thus, according to the XRD phase analysis, regardless of modifying a partial destruction of intermetallic compound Ni_3Al occurs in the course of CDMC, with the formation of free nickel, as well as of the solid solution of Al in Ni. The principal difference between the samples studied consists in the fact that the catalyst implanted with platinum is not carbonized, so it is promising from the standpoint of the stability of its operation in the CDMC process.

Structural changes of catalysts in the course of carbon dioxide methane conversion

The method of SEM revealed morphological features of the initial catalysts and catalysts developed in the process of CDMC, as well as the topographic characteristics of the condensation products deposited. According to the results of SEM and specific surface measurements, the initial sample has a macroporous ($d = 6 \cdot 10^{-5}$ and $2 \cdot 10^{-5}$ m) structure (Fig. 4, a) with a small specific surface area ($0.5 \text{ m}^2/\text{g}$), which is consistent with literature data for the systems obtained *via* the SPHTS [15].

After the catalytic experiments, the porous structure of the initial sample formed under SPHTS remains (see Fig. 4, b). To all appearance, this could be caused by a high thermal stability of alloys based on nickel aluminides [1]. However, a relatively smooth surface of the initial sample is altered to a considerable extent by the action of the reaction medium (see Fig. 4, b, c): there are loosening of the surface due to catalytic erosion, the formation of nuclei of metallic nickel phase, as well as a partial carbonization of the contact area observed. In the latter case, on different parts of

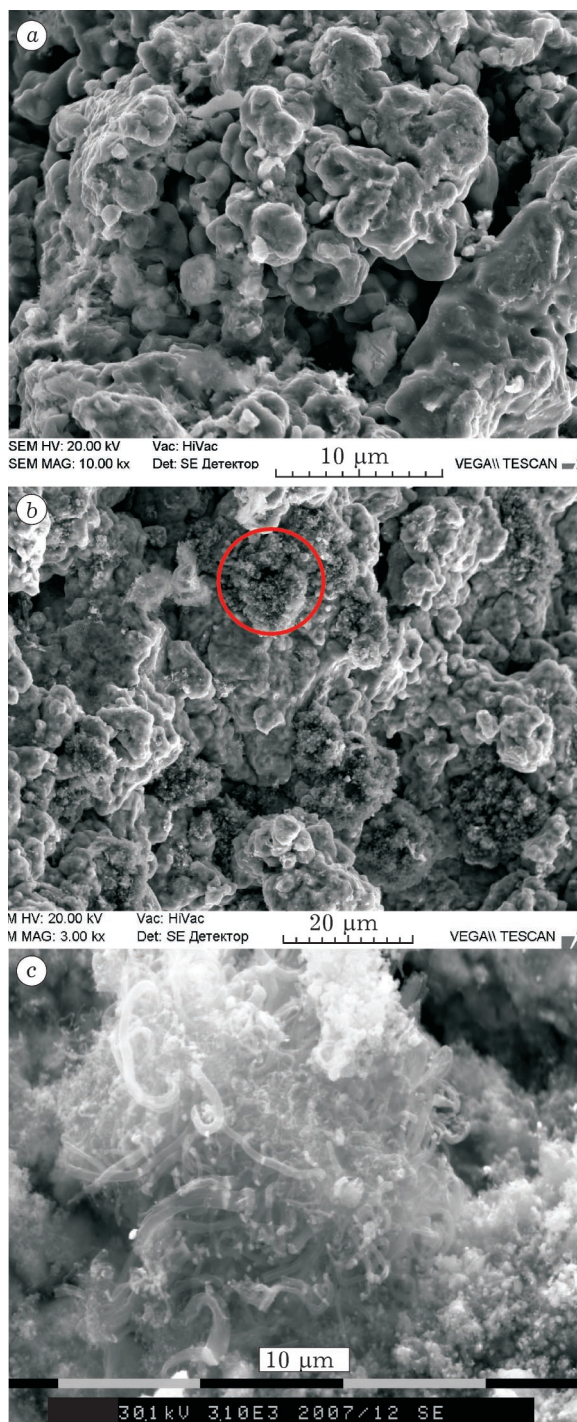


Fig. 4. Morphology of catalyst based on Ni_3Al : a – initial sample; b, c – different parts of the surface with globular carbon (b) and carbon fibres formed in the course of CDMC during 24 h at 900 °C (c).

the catalyst there are fragmented or globular clusters of carbon black (see Fig. 4, b), or carbon fibre (see Fig. 4, c), which could be caused by different nickel dispersion level on the surface formed as the result of non-equilibrium

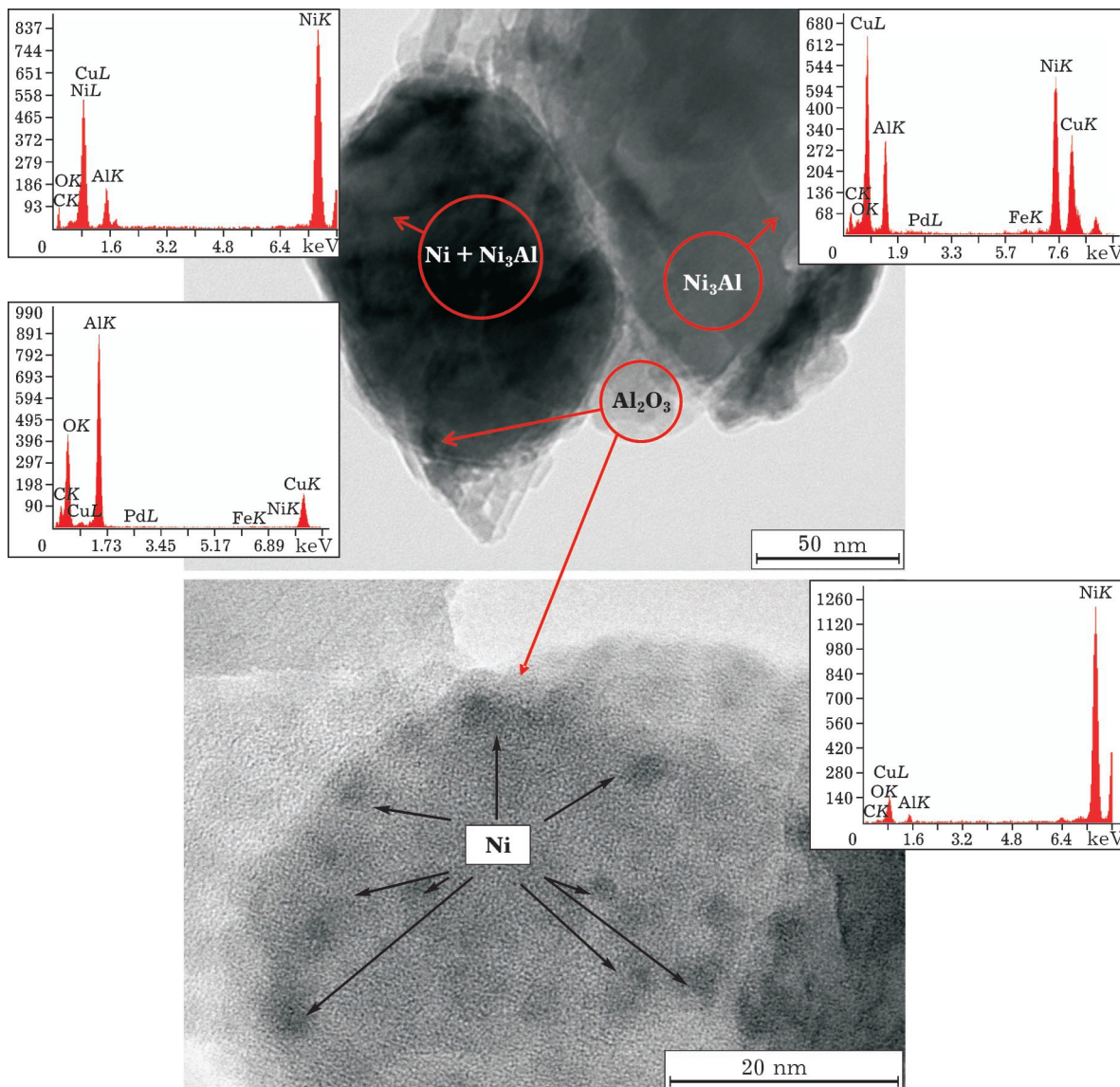


Fig. 5. HRTEM micrographs and EDX spectra of the initial catalyst based on Ni_3Al .

SPHTS method. Such a change in the surface structure explains to some extent the increase in the specific surface area observed after the catalytic experiments, amounting up to $1.9 \text{ m}^2/\text{g}$.

According HRTEM (Fig. 5), the structure of a catalyst based on Ni_3Al obtained by the SPHTS includes areas with the face-centred cubic lattice and the ordering strictly corresponding to the composition of Ni_3Al intermetallic, as well as adjacent areas with somewhat higher interplanar spacing (0.210 and 0.211 nm) and the absence of distinctly determined interfaces. To all appearance, this fact could be caused by the presence of structural

defects as well as regions with the coexistence of several phases.

For example, Fig. 5 presents fragmentary areas with the size of 100–150 nm represent two-phase catalyst areas (Ni and Ni_3Al), partially bordered by a thin film (10–20 nm) of aluminium oxide, which was, to all appearance, formed in the course of the SPHTS. At the same time, in these areas there is a large number of fine nickel particles with the size equal to 1.6 nm uniformly distributed within the matrix. The presence of thin Al_2O_3 film, firstly, provides an additional activation of CO_2 molecules, which further allows removing carbon formed

in the course of CH_4 dissociation, *i. e.*, provides inhibiting the coal formation, and secondly, the film protects nickel from further oxidation, which takes place in the course of the reforming process.

The method of XPS demonstrated that the Ni2p spectral line in the initial Ni_3Al sample can be decomposed by the deconvolution into the two components with binding energies equal to 852.04 and 855.35 eV, corresponding to Ni^0 and Ni^{2+} (such as NiO or NiAl_2O_4), whereas after the catalysis the relative Ni^{2+} signal intensity increases, *i. e.* the sample undergoes oxidation. The Al2s spectral line after the deconvolution resulted in three components: 111.58 eV (Al^0), 118.51 eV (AlO_x or Al_2O_3 , as an amorphous component, the most intense line) and 120.89 eV (NiAl_2O_4). At the same time, the third signal becomes more intense after the catalysis, *i. e.*, the surface of the sample is, to all appearance, partially oxidized not only to yield nickel oxide, but also to give spinel. It should be meant that methane does almost not react with oxidized nickel, but actively interacts with the catalyst in the reduced state to form hydrogen and surface carbon that reacts slowly with the lattice oxygen and rapidly with the adsorbed oxygen [8]. Just so rapidly CO_2 reacts with surface carbon to form CO , and slowly interacts with a metal to form CO and MO . Thus, the main route of the CDMC process includes the dissociative adsorption of methane to form $\text{C} + 2\text{H}_2$ as well as carbon interaction with CO_2 according to the reverse Boudouard reaction [8]. Side reaction routes include the interaction between the products of methane chemisorption with the oxygen of the catalyst, and CO_2 dissociative adsorption of onto a metal. The competitive reaction of the carbon surface with adsorbed oxygen reduces the conversion of CO_2 in the course of the main reaction; therefore, for example, the presence of oxygen in the reaction mixture reduces the rate of $\text{CH}_4 + \text{CO}_2$ reaction (poisoning the catalyst with oxygen). Thus, the partial deactivation of the intermetallic compound could be caused not only by carbon deposits on the surface, but also by the oxidation of the active component of nickel to give nickel oxide and spinel.

Interesting results were obtained for the platinum-modified Ni_3Al catalyst. Figure 6 demon-

strates the structure of the initial catalyst $\text{Ni}_3\text{Al} + \text{Pt}$ (the dose equal to $1 \cdot 10^{17}$ ions/ cm^2). It is seen that the surface represents a typical split of the alloy, relatively smooth, with minor irregularities, that has extensive cracks with an average width amounting to 0.1–0.5 μm . Separate fragments form weakly pronounced “steps”, each step being 0.5–2 μm in height and 1–3 μm long. There are a small number of pores with an average diameter of 1.4 μm observed as well as spikes with irregular spherical shape, with the size 2–5 μm in size.

At high temperature values and severe redox environment wherein the carbon dioxide methane reforming takes place the structure of the catalyst changes, but not as substantially as the unmodified Ni_3Al matrix does (see Fig. 6, b). After the catalysis the surface is transformed as it follows: a part (20–30 %) remains

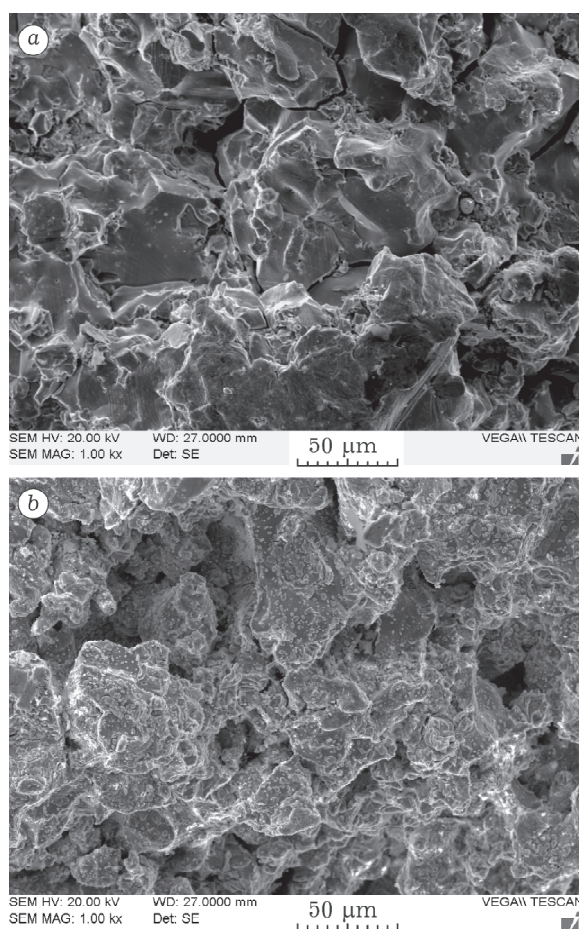


Fig. 6. Morphology of the catalyst based on $\text{Ni}_3\text{Al} + \text{Pt}$: a – initial sample, b – after the catalytic tests in the course of CDMC during 24 h at 900 °C.

without explicit changes, porosity level being conserved, however, the formation of a new phase in the form of small crystals (0.1–0.3 μm) with a clear-cut inherent in pure metals is obvious. The local elemental analysis demonstrated that these crystallites represent pure nickel, segregated to the surface from the bulk of a multiphase heterogeneous system such as Ni + Ni₃Al + the solid solution of Al in Ni. This is indicated by HRTEM data, too: Fig. 7 clearly demonstrates the crystallites of nickel (about 10 nm in size), segregated from the surface layer of the intermetallic compound being at the aggregation stage (an amorphous “isthmus” is observed between the two clusters of nickel). In this case the nearest cluster of Ni is located in focus, and a regular crystalline structure is distinctly seen, which structure exhibits a diffraction pattern with the interplanar distance amounting to 0.203 nm (the reflex from the Ni plane (111)).

In addition, the structure of the mentioned catalyst exhibits fine platinum particles to observe, ranging in size from 0.3–0.5 to 3–5 nm, stabilized mainly in the intermetallide and aluminium oxide matrix (Fig. 8). Simple estimates demonstrate that the particles of this size contain from 3–6 to 30–60 platinum atoms only.

It should be noted that highly dispersed platinum clusters formed in the course of ion implantation are characterized by a relatively high stability during heat treatment of the catalyst in the oxidation–reduction medium inherent in

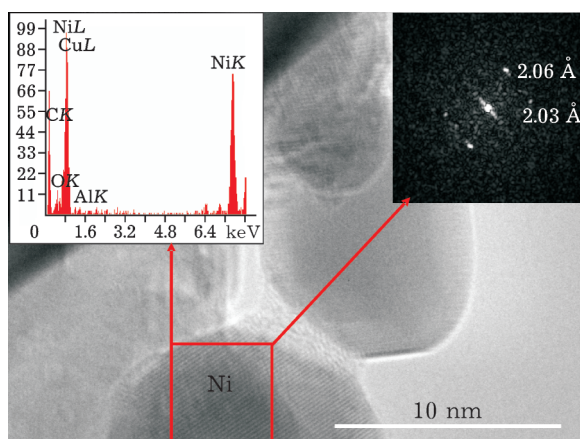


Fig. 7. HRTEM micrograph, the local EDS spectrum and Fourier diffraction pattern of the catalyst based on Ni₃Al, implanted with platinum, developed in the course of CDMC (for the process conditions see Fig. 1).

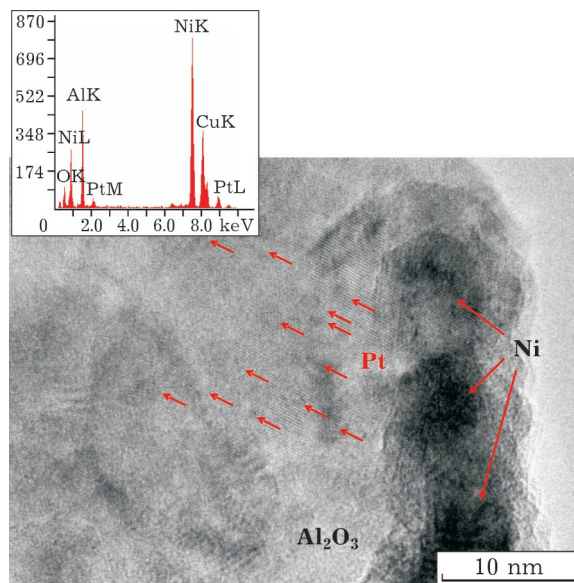


Fig. 8. HRTEM micrograph and total EDX spectrum of freshly prepared catalyst based on Ni₃Al, platinum implanted.

CDMC, *i. e.*, the Pt particle size after the tests in the methane reforming for 24 h within the temperature range 600–900 °C remains unchanged. It is noteworthy that in this case there was no carbonization of contact surfaces observed, *i. e.*, no soot or carbon fiber (as against how it was in the case of unmodified matrix) was registered. It is likely that platinum that exhibits a lower solubility of carbon as compared to nickel, promotes reducing the rate of carbon diffusion through the catalyst bed.

The studies performed demonstrate that the microstructure exerts a significant effect on the catalytic properties of the samples. For comparison, we synthesized a Ni₃Al + Pt catalyst, however, platinum was not introduced via ion implantation, but it was directly introduced in the course of the SPHTS. In this case the mass fraction of platinum was 3 %, which is an order of magnitude higher than that after implantation as calculated for the specific mass of the sample (with no taking into account any surface and volume distribution). As the result, the catalytic parameters were comparable with those for implanted samples, although CH₄ and CO₂ conversion level values were 2–6 % lower, depending on the conditions of CDMC. To all appearance, this fact could be caused by a reduced concentration of surface Pt atom, avail-

able for the adsorption of methane. In addition, the catalyst was prone to local carbonization.

Stability and deactivation

The stability test was carried out in the course of methane conversion into synthesis gas at the temperature value amounting to 900 °C during 140 h, at a molar ratio $\text{CH}_4/\text{CO}_2 = 1 : 1$ (Fig. 9). The $\text{Ni}_3\text{Al} + \text{Pt}$ catalyst worked steadily during the first 65–70 h, no development time was fixed, further there is a weekly pronounced decrease in activity observed, with the conversion level decreased only by 2–4 %.

Despite a very low content of platinum (implantation dose of $1 \cdot 10^{17}$ ions/cm²), the stability of the implanted catalyst is much higher than the stability of the matrix. This could be explained by extremely low carbon solubility in precious metals, as well as dispersing the platinum onto the entire surface of the sample. Bombarding the crystal structure (formed within the surface layer) with accelerated platinum ions results in the layer damage such as the generation of defects, vacancies and other types of lattice disordering, in the regions around an ion track. With increasing the number of ions hitting Ni_3Al grain in the course of implantation, individual disordered regions begin overlapping to the formation highly distorted layers. The total change in the lattice structure and damage distribution of over the depth depend to a considerable extent on the ion charge (Pt^{2+} , Pt^{4+}), target temperature, ion energy, total dose as well as on the channelling effect [13]. (The latter could be neglected due to the absence of axial and planar channels in multiphase polycrystalline samples, based on Ni_3Al obtained under the non-equilibrium conditions of SPHTS.) As a consequence, at the surface region of material produced there are atomic mixtures formed, whose composition is not limited by the principles of thermodynamics, whereas nickel clusters are divided into much smaller size subclusters those are to a less extent prone to carbonization [8, 12].

For the unmodified catalyst based on Ni_3Al , within the first 6–12 h the conversion level values for CO_2 and CH_4 exhibit a slight increase (during the development time), then the catalyst is stable for 35–40 h, and only after 50–

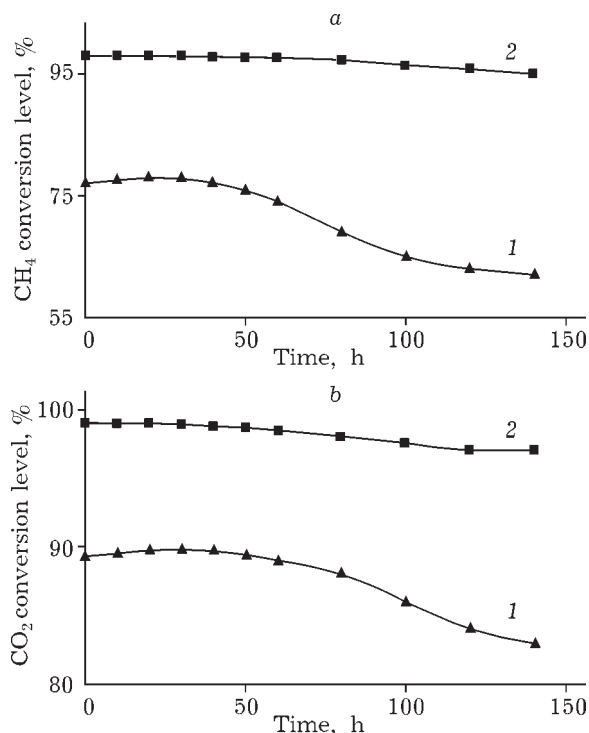


Fig. 9. Conversion level of methane (a) and carbon dioxide (b) depending on time for catalysts Ni_3Al (1) and $\text{Ni}_3\text{Al} + \text{Pt}$ (2).

55 h of the conversion level values for both components decrease. This is could be mainly connected with the carbon deposition on the contact surface with a partial oxidation of nickel.

In principle, the deactivation could be caused by several factors such as a decrease in the number of active centers due to sintering the particles of the catalyst active phase, interaction between active metals and the carrier in the solid phase, and carbon deposition. According to microscopic studies, no sintering the intermetallics based heat-resistant Ni_3Al matrix was detected. Using the XPS, we registered the effect of interaction with the carrier resulting in the formation of NiAl_2O_4 on the catalyst surface; at the same time, it is known that spinel uses to suppress carbon deposition. Finally, the methods of XRD, SEM (+EBB), TEM, DTA-TG revealed the carbonization of unmodified Ni_3Al matrix.

In this paper we identified two forms of carbon deposits (see Fig. 4, b, c) such as globular and fibrous one. A more detailed study with the use of TEM (HRTEM) demonstrated that the structure features of the carbon deposits are very different from each other (Fig. 10). The

carbon tubes exhibit a bamboo-like (see Fig. 10 *a, b*) and coaxial conical structure with the outstation of Ni particles into the structure of the carbon fibre (see Fig. 10, *c*). In addition, there is carbon deposition observed with a loose, low-ordered structure, wherein carbon is composed of separate fragments of graphite-like phase (see Fig. 10, *g*).

In the first case, the particles of nickel are coated by graphite with $\langle 002 \rangle$ interplanar distance 0.348 nm. This value somewhat differs from the ideal distance for graphite (0.336 nm) being close to interplanar distances for other carbon materials, such as Sibunit (0.348 nm) and technical carbon (0.362 nm) capable of intercalation. However, in this case, the removal of metal from the catalyst surface is not accompanied by its intercalation to between the graphite layers. Figure 10, *b* clearly demon-

strates that the basal planes of graphite formed during the methane catalytic reaction with carbon dioxide are oriented parallel to the surface of metal (nickel, according to EDS) particles. At the same time, the thickness of the graphite structures amounts up to 30–50 nm, *i. e.*, several tens (sometimes more than 100) of basal (almost defectless) graphite planes.

The reasons for the formation of bamboo-like tubes could be explained from the standpoint of cyclic changes in the supersaturation level of catalyst particles by carbon immediately at the contact area with growing carbon nanotubes [18]. It is known that the rate determining stage in the growth of carbon nanotubes consists in the diffusion of carbon through a metal particle [19, 20]. We can assume that after the formation of carbon on the surface of a critical nucleus, the growth of the pri-

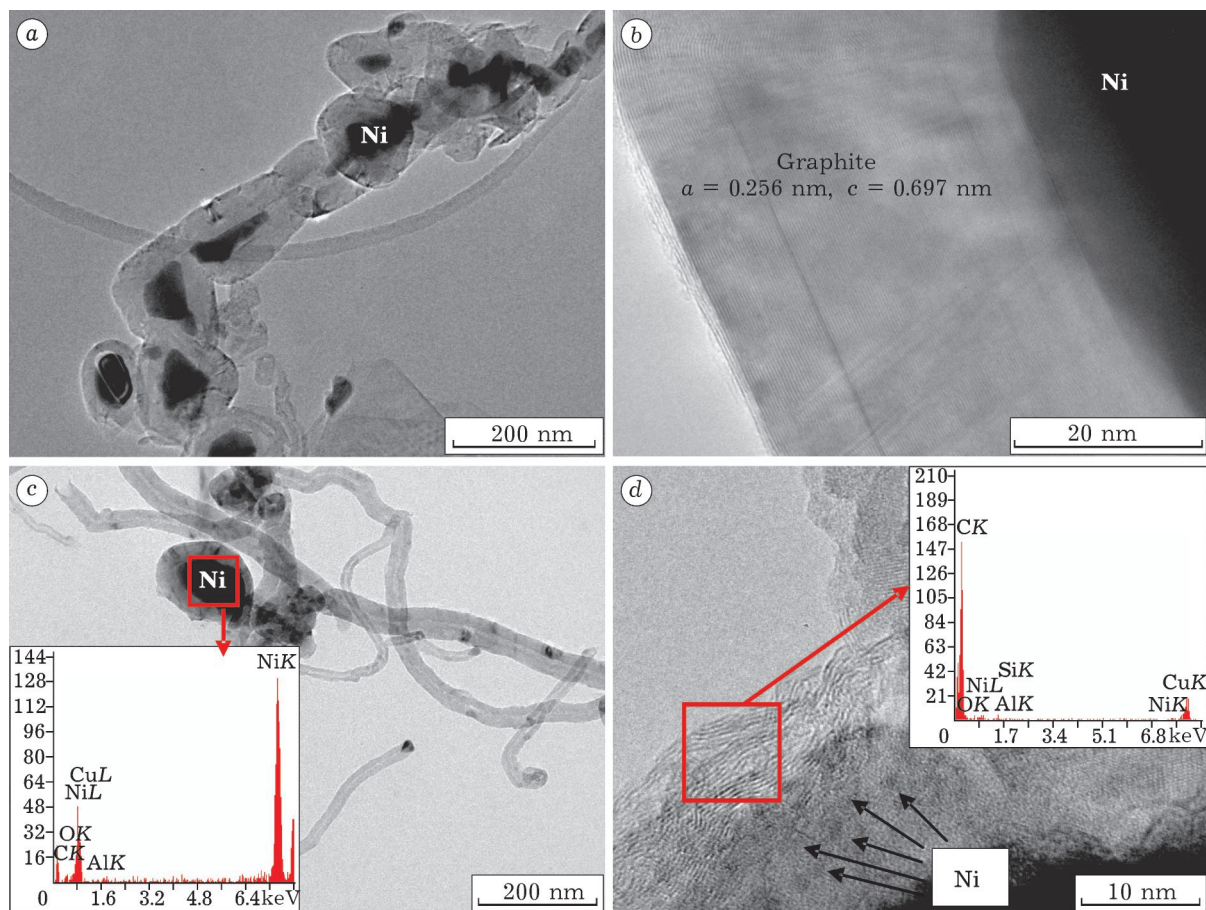


Fig. 10. Carbon deposits on the surface of catalyst based on Ni_3Al , formed in the course of CDMC during 24 h at 900 °C: *a, b* – bamboo-like structure, *c* – coaxial conical, *d* – the fragments of predominantly amorphous low-ordered graphite structure.

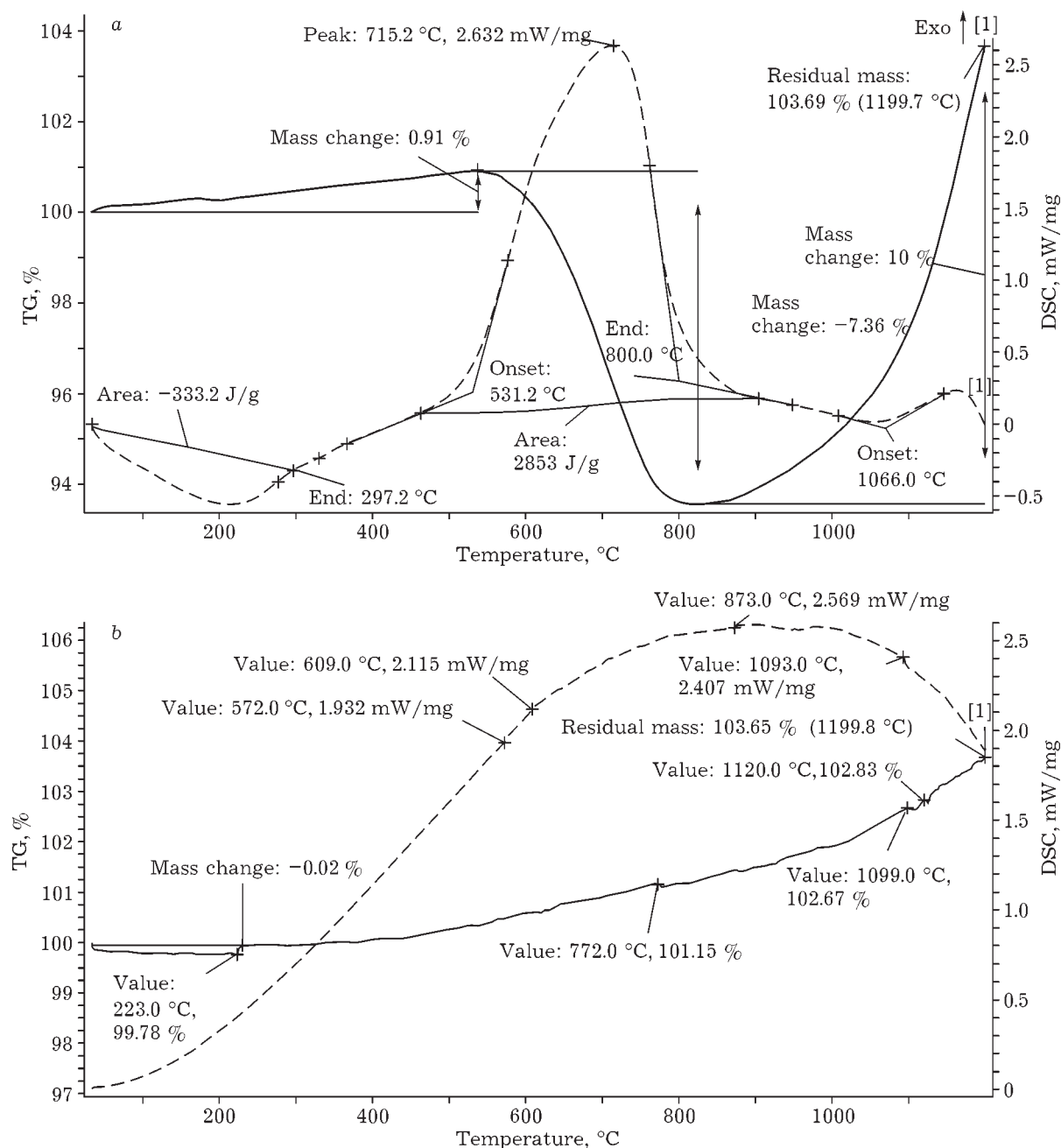


Fig. 11. DSC-TG curves for catalysts based on Ni₃Al (a) and implanted with platinum (b) after testing in the course of CDMC during 24 h at 900 °C.

mary nucleus occurs, where under new nuclei are successively formed and grow, and this results in the formation of multiple graphene layers. The concentration of carbon atoms in the surface layer of the metal decreases abruptly, since the diffusion rate of carbon atoms is low. This is possible under transient conditions, when the flow of carbon diffusing within the metal

particles is smaller than the flux of carbon that providing the growth of the tube.

Each value of the supersaturation level corresponds to a certain critical radius of the nucleus [18], so the decrease of supersaturation would cause an increase in the critical radius for the next nucleus. The formation of a new nucleus with the radius greater than the radi-

us of inner tube channel should be impossible. Under these conditions, an introduction of carbon atoms should occur through the metal-carbon bonds at the edges of the growing nucleus and, therefore, the growth of hollow carbon tube should be observed. The further growth of the tube will occur until the time to achieve carbon supersaturation within the surface layer of the metal (due to the diffusion of carbon atoms), which supersaturation is sufficient in order to form a new nucleus with the critical radius value less than or equal to the tube channel. After growing the nucleus which represent a partition wall in growing tube, reducing the carbon content in the surface layer occurs, as well as the growth of the tube and subsequent saturation of the particles by carbon to a value sufficient for the appearance of a nucleus with the critical radius less than or equal to the channel of the tube. Most likely, the main reason for the formation of the “bamboo-like” carbon tubes consists in periodic changing the supersaturation of metal particles with carbon [18].

The formation of condensation products was quantitatively evaluated according to the DTA-TG data. Depending on the time of operation for unmodified catalyst based on Ni₃Al in CDMC process in, as well as on the CDMC process temperature, the increase in the mass due to carbonization averaged from 0.3 to 12 %. This is in a good agreement with the XRD data for the samples developed during an extended period (more than 24 h), when not only amorphous, but graphite-like carbon detected by XRD is formed in the course of CDMC. Figure 11, *a* demonstrates DTA-TG data obtained under thermo-programmed air oxidation of the based on Ni₃Al catalyst developed within 24 h in the course of CDMC.

The diffuse endothermic effect within the range of low temperature values (lower than 250 °C) could be caused by desorption of water adsorbed from atmospheric air. A negligible increase in mass on the TG curve prior to 500 °C could be caused by a gradual oxidation of nickel (with a small delay within the region of water desorption). An abrupt change in mass on the TG curve, accompanied by a significant exothermic effect in accordance with the reaction $C + O_2 = CO_2$, $\Delta H_f^\circ = -393.51 \text{ kJ/mol}$ within the temperature range of 530–800 °C, could be caused by the combustion of conden-

sation products formed during the catalytic experiments, with the formation of CO₂ (confirmed by mass-spectrometric studies). Taking into account the existence of different carbon forms on the surface of coked catalyst the asymmetry of the exothermic effect could be caused by the combustion of amorphous carbon at the first stage, which amorphous carbon is, as a rule, oxidized first among various modifications of carbon [3, 4, 12], whereas the second stage is characterized by burning out the products of condensing the graphite-like structure.

The total amount of carbon deposition products was equal to 7.36 mass % of weighed catalyst portion. The further sharp increase in the mass of the sample at the temperature of 800 °C characterizes the process of nickel oxidation in the reaction



which is accompanied by an exothermic effect on the DSC curve.

For the modified platinum intermetallic compound Ni₃Al, DTA-TG curves were obtained indicating the absence of the carbon deposits for a sample developed in the course of CDMC under similar conditions (see Fig. 11, *b*). A slight increase in the sample mass under thermo-programmed heating in air at 400 °C, accompanied by a weakly pronounced diffuse exothermic effect could be caused by a gradual nickel oxidation to the oxide.

Thus, the introduction of platinum exerts a favourable effect not only on the catalytic parameters of the Ni-Al system, but also inhibits to a considerable extent the process of carbon deposition onto the contact surfaces preventing them from deactivation.

CONCLUSION

Thermal stability, mechanical strength, high thermal conductivity and the specific structure of superalloy Ni₃Al determine its applicability as a catalyst in the reaction of carbon dioxide methane conversion, giving rise to obtaining environmentally appropriate fuel such as dimethyl ether.

The principal difference of the catalyst used in this work from the majority of catalysts described in the literature for the process of methane conversion into synthesis gas consists in the

nature of a carrier. In this case, not metal oxide, but intermetallic compound Ni_3Al serves as the carrier, whose structure includes nickel clusters, the effective centers for the activation of methane and carbon dioxide.

Under the conditions of high temperature (850–900 °C) and severe redox media inherent in the course of carbon dioxide methane conversion, the surface of the catalyst based on Ni_3Al undergoes a partial blockage by carbon deposition products, present in the two forms such as globular and fibrous one. Carbon filaments exhibit bamboo-like and coaxial conical structure with the outstation of Ni particles to the structure fibres.

The modification of the catalytic system based on Ni_3Al , with platinum at very low concentrations by ion implantation improves to a considerable extent not only the catalytic activity, but also the stability of the catalyst over time, since platinum exhibits catalytic activity with respect to CDMC, whereas being introduced in such a manner that the platinum is in a highly dispersed state. In addition, platinum promotes an increase the dispersion level of nickel and a deceleration of the diffusion of carbon formed in the course of methane and carbon dioxide dissociative adsorption. This prevents the formation of nickel carbides and, therefore, carbon deposition is caused to reduce to a considerable extent.

The work performed has demonstrated that the ion implantation represents a promising way to effectively modify physicochemical and catalytic properties of materials.

Acknowledgement

The author is grateful to Yu. S. Nayborodenko and N. G. Kasatsky for their help in the synthesis of

catalysts, E. M. Oksu and K. P. Savkin for the help with ion implantation and A. N. Shmakov for his help in the interpretation of XRD data

REFERENCES

- 1 Itin V. I., Nayborodenko Yu. S., Vysokotemperaturny Sintez Intermetallicheskikh Soyedineniy, Izd-vo TGU, Tomsk, 1989.
- 2 Arkatova L. A., Kurina L. N., *Rus. J. Phys. Chem.*, A 84 (1) (2010) 19–24.
- 3 Arkatova L. A., *Rus. J. Phys. Chem.*, A 84, 4 (2010) 566.
- 4 Arutyunov V. S., Krylov O. V., *Okislitelnye Prevrashcheniya Metana*, Nauka, Moscow, 1998.
- 5 Bradford M. C. J. and Vannice M. A., *Catal. Rev.-Sci. Eng.*, 41, 1 (1999) 1.
- 6 Khallish D., Sherifi O., Ben-Taarit O., Oru A., *Kinetika i Kataliz*, 49, 5 (2008) 698.
- 7 Wang Sh. and Lu G. Q., *Ind. Eng. Chem. Res.*, 38 (1999) 2615.
- 8 Krylov O. V., *Ros. Khim. Zh.*, 44, 1 (2000) 19.
- 9 Juan-Juan J., Roman-Martinez M. C., Illan-Gomes M. J., *Appl. Catal. A: Gen.*, 355 (2009) 27.
- 10 Ma Y., Xu Y., Demura M., Hirano T., *Appl. Catal. B.*, 80 (2008) 15.
- 11 Arkatova L. A., Kurina L. V., Galaktionova L. V., *Rus. J. Phys. Chem. A*, 83, 4 (2009) 624.
- 12 Arkatova L. A., *Catal. Today J.*, 157 (2010) 170.
- 13 Lyakishev N. P. (Ed.), *Fazovye Diagrammy Sostoyaniya Dvoynkh Metallicheskikh Sistem*, vol. 1, Mashinostroeniye, Moscow, 1996.
- 14 Didenko A. N., Sharkeev Yu. P., Kozlov E. V., Ryabchikov A. I., *Effekty Dalnodeystviya v Ionno-Implantirovannykh Materialakh*, Izd-vo NTL, Tomsk, 2004.
- 15 Zavyalova U. F., Tretyakov V. F., Burdeynaya T. N., Lunin V. V., Shitova N. B., Ryzhova N. D., Shmakov A. N., Nizovskiy A. I., Tsyurulnikov P. G., *Kinetika i Kataliz*, 46, 5 (2005) 795.
- 16 Arkatova L. A., *Zauglerozhivaniye i Regeneratsiya Mednykh i Serebryanykh Katalizatorov Protsessa Okisleniya Etilenglikolya v Glioksal* (Candidate's Dissertation in Chemistry), TGU, Tomsk, 2000.
- 17 Vaks V. G., *Soros. Obraz. Zh.*, 3 (1997) 115.
- 18 Kuznetsov V. L., Usoltseva A. N., Butenko A. Yu., *Kinetika i Kataliz*, 44, 5 (2003) 791.
- 19 Baker R. T. K., Barber M. A., Harris P. S., Feates F. S., and Waite R. J., *J. Catal.*, 26 (1972) 51.
- 20 Buyanov R. A., *Zakoksovaniye Katalizatorov*, Nauka, Novosibirsk, 1983.